

Supporting information

**Boosting the Long-Term Stability of Hydrotalcite-Derived Catalysts
in Hydrogenolysis of Glycerol by Incorporation of Ca(II)**

Honghui Gong,[†] Xiuge Zhao,[†] Xiyu Li,[†] Manyu Chen,[†] Yuan Ma,[†] Jian Fang,[†] Xinjia
Wei,[†] Qingpo Peng,[†] and Zhenshan Hou^{*,†}

[†]Key Laboratory for Advanced Materials, Research Institute of Industrial Catalysis,
School of Chemistry & Molecular Engineering, East China University of Science and
Technology, 130 Meilong Road, Xuhui District, Shanghai 200237, China.

Corresponding author: E-mail: houzhenshan@ecust.edu.cn

Number of Pages: 22

Number of Figures: 11

Number of Tables: 3

Table of contents

Experiment Section	S3
Table S1	The composition of crude glycerol.....	S8
Figure S1	XRD patterns of HT precursors and CaCO ₃	S9
Figure S2	FT-IR spectra of the samples.....	S10
Figure S3	SEM images of the catalysts.....	S11
Figure S4	Influence of various reaction parameters on the catalytic performance.....	S12
Figure S5	The recyclability of Co ₆ -Al ₃ catalyst.....	S13
Figure S6	XRD patterns of the spent catalysts.....	S14
Figure S7	SEM images of the spent catalysts.....	S15
Figure S8	TGA curves of catalysts.....	S16
Table S2	Comparison of the Co ₂ -Ca ₄ -Al ₃ catalyst with reported catalytic systems.....	S17
Figure S9	(a) XRD patterns of the Co ₂ -Ca ₄ -Al ₃ _OH_HT and Co ₂ -Ca ₄ -Al ₃ _OH. (b) H ₂ -TPR profiles of the Co ₂ -Ca ₄ -Al ₃ _OH_HT. (c) CO ₂ -TPD profiles of Co ₂ -Ca ₄ -Al ₃ _OH catalyst.....	S18
Table S3	The hydrogenolysis of glycerol on various catalysts.....	S19
Figure S10	The recyclability of Co ₂ -Ca ₄ -Al ₃ _OH catalyst.....	S20
Figure S11	(a) XRD patterns of the Co ₂ -Ca ₄ -Al ₃ _Ox catalysts; (b) Co 2p XPS spectrum of the Co ₂ -Ca ₄ -Al ₃ _Ox catalyst.....	S21
Reference	S21

Experimental Section

Materials

All the materials and reagents were commercially available and were not purified further prior to use. Cobalt nitrate hexahydrate ($\text{Co}(\text{NO}_3)_2 \cdot 6\text{H}_2\text{O}$, 99%) was supplied by Macklin Biochemical Co., Ltd. Sodium hydroxide (NaOH, 97%), and sodium carbonate anhydrous (Na_2CO_3 , 99%) were bought from Aladdin Industrial Corporation. Calcium nitrate tetrahydrate ($\text{Ca}(\text{NO}_3)_2 \cdot 4\text{H}_2\text{O}$, 99%), aluminium nitrate ($\text{Al}(\text{NO}_3)_3 \cdot 9\text{H}_2\text{O}$, 99%) were provided by Shanghai Lingfeng Chemical Reagent Co., Ltd. High purity N_2 (99.999%) and H_2 (99.999%) was supplied by Shanghai Pujiang Specialty Gases Co., Ltd. Crude glycerol was directly purchased from Hebei Fucheng Chemical Co., Ltd without any further purification. The composition of crude glycerol aqueous solution utilized in this study was shown in Table S1. It can be seen that the crude glycerol used in this study has 50.2 wt % glycerol content and is accompanied by water (47.3 wt %), MONG (1.45 wt %) as main impurities, as well as high content of sodium (559 ppm) probably due to the catalyst (NaOH) employed in biodiesel production. All other chemicals were bought from Sino pharm Chemical and used without further purification.

Catalysts Preparation

The Co-Ca-Al_{HT} with different molar ratios of Co:Ca:Al were prepared by concurrent-precipitation method according to the following procedure. In a typical example, the required amounts of M^{2+} ($\text{Co}(\text{NO}_3)_2 \cdot 6\text{H}_2\text{O}$ and/or $\text{Ca}(\text{NO}_3)_2 \cdot 4\text{H}_2\text{O}$, 0.06 mol) and M^{3+} ($\text{Al}(\text{NO}_3)_3 \cdot 9\text{H}_2\text{O}$, 0.03mol) were dissolved in 120 mL distilled water under stirring, and this solution was referred as A, in which $\text{M}^{2+}/\text{M}^{3+} = 2$ and the total molar amount of metal ions (including M^{2+} and M^{3+}) is 0.09 mol. Solution B containing NaOH (0.21 mol) and Na_2CO_3 (0.089 mol) was dissolved in 120 mL distilled water. Then solution A and B were added slowly to a 500 mL three-necked flask under vigorously stirring at room temperature, the pH was maintained at 10 during dripping process. The resulted suspension processed at 75°C for 1 h and then stopped stirring

and aging at this temperature for 18 hours. After aging, the precipitate was filtered, followed by washing thoroughly with distilled water until the pH of filtrate reached 7.0. The obtained precipitate was then dried at 80°C for 12 h to obtain pink powder and designated as Co_{6-x}-Ca_x-Al₃_HT, where x referred to the molar ratios of Ca(II) and was equal to 0-5, respectively. The resulting material was calcined in a reduction atmosphere (H₂/N₂=1/9, v/v) at 600°C (heating rate: 5°C·min⁻¹) for 2 h. After the catalyst was cooled to room temperature, it was then passivated by mixed gas (O₂:N₂=1:99, v/v) for 2 h to achieve the corresponding catalysts, which were named as Co_{6-x}-Ca_x-Al₃. For the sake of comparison, Co₂-Ca₄-Al₃_Ox was prepared by re-oxidation of Co₂-Ca₄-Al₃ at 300°C for 2 h in air.

To investigate the effect of interlayer anions of CO₃²⁻, the Co₂-Ca₄-Al₃_OH_HT was also prepared by the same method as Co₂-Ca₄-Al₃_HT, except that there was no Na₂CO₃ in solution B and the material was synthesized in a flow of N₂. The resulting catalyst was named as Co₂-Ca₄-Al₃_OH after the Co₂-Ca₄-Al₃_OH_HT was calcined under a reduction atmosphere (H₂/N₂=1/9, v/v) at 600°C. Besides, CaCO₃ was also prepared by concurrent-precipitation method. 50 mL of aqueous solution containing 1.78 M Na₂CO₃ was added slowly to 50 mL aqueous solution containing 0.4 M Ca(NO₃)₂·4H₂O under vigorously stirring at room temperature, the pH was maintained at 10 during dripping process. The resulted suspension processed at 75°C for 1 h and then stopped stirring and aging at this temperature for 18 hours. The resulted suspension was filtered, followed by washing thoroughly with distilled water until the pH of filtrate reached 7.0. The obtained precipitate was then dried at 80°C for 12 h and calcined at 600°C (heating rate: 5°C·min⁻¹) for 2 h to obtain white powder and designated as CaCO₃.

Catalyst Characterization

X-ray diffraction (XRD) analysis of the samples were performed in the 2θ range of 5°-75° on an Rigaku D/MAX 2550 VB/PC instrument using Cu Kα radiation. The textural properties from N₂ adsorption isotherms were obtained on Quanta chrome NOVA 2200e equipment. BET surface area and pore structure were calculated on adsorption branch. The inductively coupled plasmaatomic emission spectroscopy (ICP-

AES) analysis was carried out on a Varian ICP-710ES instrument. The sample was putted in a plastic beaker mixed with a certain amount of aqua regia at 80°C for 2 h, followed by diluted with water. Temperature-programmed reduction (H₂-TPR) was performed using VDSorb-91i. The catalyst was placed in a U-shaped quartz tube, then purged under pure Ar (10 mL·min⁻¹) flow at 400°C for 2 h, and then cooled down to 20°C. After that, it was reduced with H₂/Ar (1/9, v/v) (10 mL·min⁻¹) up to 900°C (ramp rate of 10°C·min⁻¹). A cooling trap was employed to condense the minor water vapor before the carrier gas flowed into the TCD detector in H₂-TPR analyses. The thermal stability of catalysts was determined by Thermogravimetry analysis (TGA) method (heating rate: 10°C·min⁻¹; air flow, 100 mL·min⁻¹) using PerkinElmerPyris Diamond Analyser. The Scanning electron microscopy (SEM) images were performed on GeminiSEM 500. High resolution transmission electron microscopy (HRTEM) was performed in a JEOL JEM 2100 transmission electron microscope operating at 200 kV with a nominal resolution of 0.25 nm. The samples for HRTEM were prepared by dropping the aqueous solutions containing the catalysts onto the carbon-coated Cu grids. Energy dispersive X-ray spectroscopy (EDS) was carried out using 4 in-column Super-X detectors. X-ray photoelectron spectroscopy (XPS) was performed using Thermo ESCALAB 250. The basicity of Co-based catalysts was carried out via temperature-programmed desorption of CO₂ (CO₂-TPD). Samples were first pretreatment at 300°C in purified Ar flow of 30 mL·min⁻¹ for 1 h, and then cooled to 100°C, exposed to 50% CO₂/Ar for 30 min, purged by Ar for 5 h at 100°C in order to eliminate the physical adsorbed CO₂. Temperature-programmed desorption (TPD) was conducted by ramping to 800°C (heating rate: 10°C·min⁻¹) and CO₂ (m/e=44) in effluent was detected and recorded as a function of temperature by a quadrupole mass spectrometer (OmniStar™, GSD301, Switzerland).

The adsorption states of glycerol on catalysts were studied on a Nicolet Magna 550 FT-IR spectrometer. The spectrum of sample without absorbed glycerol was recorded as background. The FT-IR spectra of the Co-based catalysts after introducing glycerol (2.0 mmol g⁻¹) were carried out according to the following procedure: a mixture of glycerol (0.2 mmol), H₂O (2.0 mL) and the catalysts (0.1 g) were placed in

a 25.0 mL Schlenk flask and stirred for 1 h, followed by drying under the vacuum for 2 h at 70°C. The resulting sample was subjected to FT-IR measurement.

Catalytic Reactions

In a batch-wise reaction, a 50 mL stainless steel autoclave was used and equipped with a thermoelectric couple. Aqueous solution of substrates (15.0 mL, 20 wt % for glycerol and other sugar alcohols but 5 wt % for glucose unless otherwise indicated) and 0.5 g catalysts were added to the reactor. The reactor was purged three times with N₂ to replace the air in the autoclave, and then three times with pure H₂ to replace the N₂. Finally, hydrogen was added to the given pressure and the reactor was heated to the given temperature under vigorously stirring. When the hydrogenation reaction was carried out under low pressure (<2.0 MPa), hydrogen was supplied continuously to the autoclave through a single-way valve during the reaction. After the reaction was finished, the reactor was quenched in an ice-water bath to stop the reaction and then the catalyst was filtrated to separate from the solution before analysis. The liquid products were qualitatively analyzed by an Agilent 6890/5973 GC-MS system equipped with a HP-5MS column (30 m long, 0.25 mm i.d., 0.25 μm film thickness) and flame ionization detector (FID). For quantitative measurements, analysis was performed on a GC128 gas chromatograph equipped with an FFAP capillary column (30 m long, 0.32 mm i.d., 0.33 μm film thickness) and 1-butanol was used as the internal standard. High performance liquid chromatography (HPLC) equipped with a refractive index detector in series with SilGreen H column (300 mm × 7.8 mm) together with a guard cartridge was also employed for product analysis (e.g. LA). The column oven temperature was 50°C, the mobile phase was diluted with a concentration of 5 mM H₂SO₄ aqueous solution and 0.5 mL·min⁻¹ flow rate, 20 μL of each sample was injected and peaks were detected with refractive index detector. The gaseous products were collected and analyzed by offline GC with thermal conductivity detector (TCD). To examine the recyclability of the optimized catalyst, the catalyst was separated from the reaction mixture by filtration, following by washing three times with distilled water and three times with EtOH, respectively. Finally, the resulting material was then dried at 80°C for

3 h, which was added to a fresh reaction solution for the next run.

To further evaluate the long-term stability of the catalyst, the hydrogenolysis of glycerol was also carried out in a vertical fixed-bed stainless-steel reactor (1.1 cm i.d., length 60 cm). The solid catalyst was tableted and then crushed and sieved to 20-40 mesh particles for the catalytic reaction tests. A constant weight (2.0 g) of catalyst layer was sandwiched in the middle of the reactor with quartz wool and quartz sand for supporting the catalyst and evaporation of the reactants. The temperature was controlled by a thermocouple placed in the middle of the catalyst bed. When the temperature of reactor was constant, the feedstock, an aqueous solution containing 20 wt % glycerol, was then pumped into the reactor ($0.04 \text{ mL} \cdot \text{min}^{-1}$) and driven through the catalyst bed by hydrogen flow ($15 \text{ mL} \cdot \text{min}^{-1}$). The reaction products were condensed in a cryogenic cooling system and collected every 10 h for offline analysis. For quantitative measurements, 1-butanol was used as the internal standard. The gaseous products were also collected and analyzed by offline GC with thermal conductivity detector (TCD). The conversion of substrate was calculated using equation S1.

$$\begin{aligned} & \text{Conversion(\%)} \\ &= \frac{\text{amount of substrate reacted (mole)}}{\text{total amount of substrate used in the reaction (mole)}} \times 100\% \end{aligned} \quad (\text{S1})$$

Product selectivity and yield were calculated using equations S2 and S3.

$$\text{Selectivity (\%)} = \frac{\text{carbon in a product defined (mole)}}{\text{carbon in substrate reacted (mole)}} \times 100\% \quad (\text{S2})$$

$$\text{Yield (\%)} = \frac{\text{Conversion(\%)} \times \text{Selectivity (\%)}}{100} \quad (\text{S3})$$

Table S1. The composition of crude glycerol (brown color) utilized in this study.

Parameter	Unit	Content
Glycerol content	% w/w	50.20%
MONG	% w/w	1.45%
Ash Content (550 °C)	% w/w	0.68%
Water content	% w/w	47.30%
pH at 25°C	-	6.8
Sodium content	ppm	559

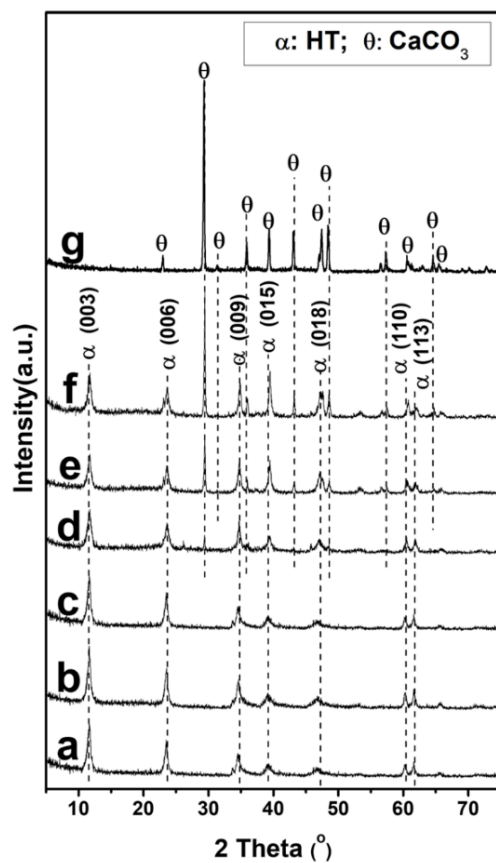


Figure S1. XRD patterns of (a) $\text{Co}_6\text{-Al}_3\text{_HT}$; (b) $\text{Co}_5\text{-Ca}_1\text{-Al}_3\text{_HT}$; (c) $\text{Co}_4\text{-Ca}_2\text{-Al}_3\text{_HT}$; (d) $\text{Co}_3\text{-Ca}_3\text{-Al}_3\text{_HT}$; (e) $\text{Co}_2\text{-Ca}_4\text{-Al}_3\text{_HT}$; (f) $\text{Co}_1\text{-Ca}_5\text{-Al}_3\text{_HT}$; (g) CaCO_3 .

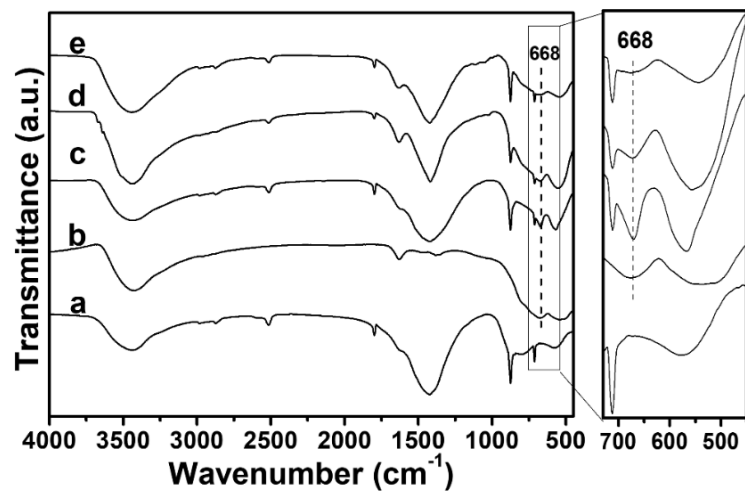


Figure S2. FT-IR spectra of the samples. (a) CaCO_3 ; (b) $\text{Co}_6\text{-Al}_3$; (c) $\text{Co}_3\text{-Ca}_3\text{-Al}_3$; (d) $\text{Co}_2\text{-Ca}_4\text{-Al}_3$; (e) $\text{Co}_1\text{-Ca}_5\text{-Al}_3$.

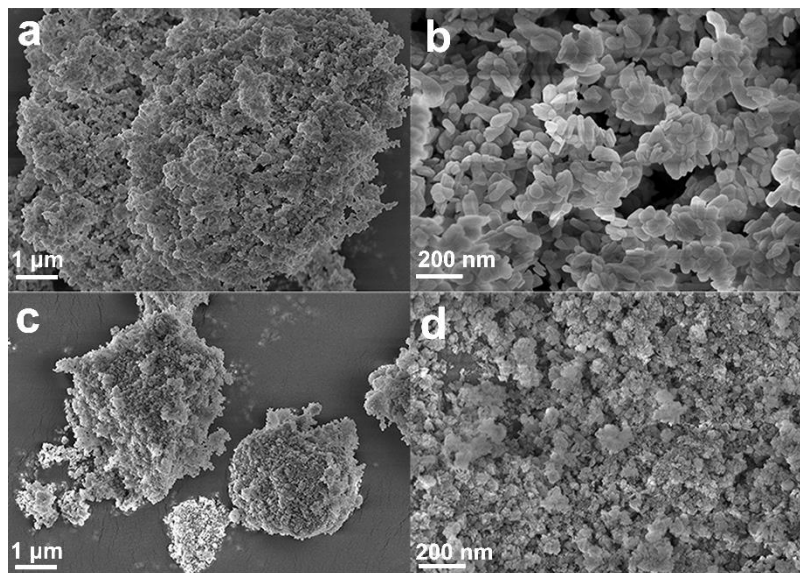


Figure S3. SEM images of the catalysts. (a, b) $\text{Co}_6\text{-Al}_3$; (c, d) $\text{Co}_2\text{-Ca}_4\text{-Al}_3$.

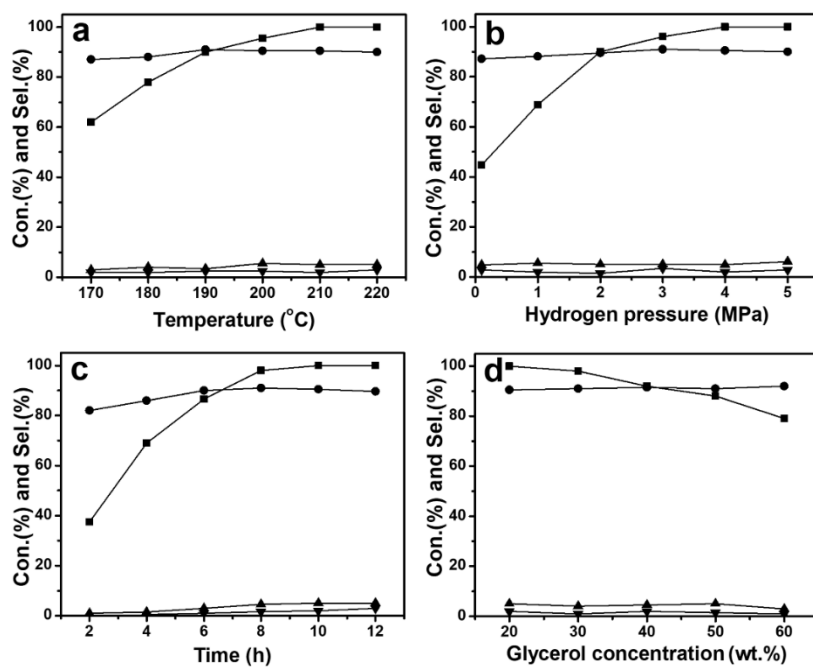


Figure S4. Influence of (a) temperature; (b) H₂ pressure; (c) time evolution and (d) glycerol concentration on the catalytic performance of Co₂-Ca₄-Al₃ catalyst in the hydrogenolysis of glycerol. (■) glycerol conversion; (●) 1,2-PDO selectivity; (▼) MeOH selectivity; (▲) EG selectivity. 15.0 mL 20 wt % glycerol aqueous solution, 0.5 g catalyst, 4.0 MPa H₂, 10 h.

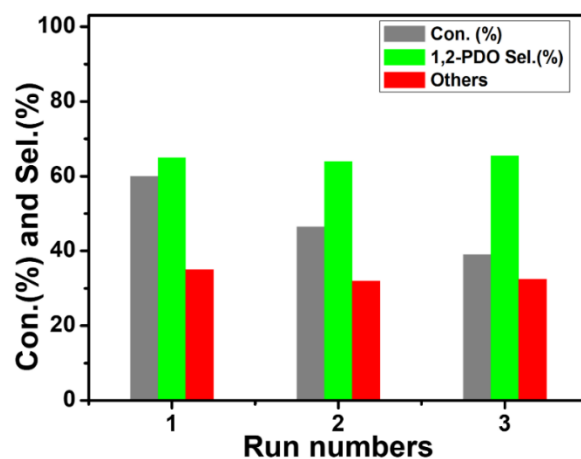


Figure S5. The recyclability of Co₆-Al₃ catalyst for selective hydrogenolysis of crude glycerol. Others: EG, MeOH, 2-PO, CO₂, CO, CH₄ and other unidentified products. Reaction conditions: 15.0 mL crude glycerol aqueous solution (50.2 wt %), 0.5 g catalyst, 4.0 MPa H₂, 210 °C, 10 h.

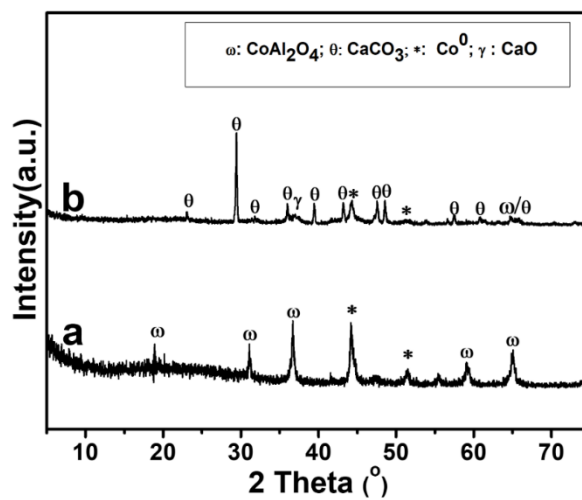


Figure S6. XRD patterns of the spent catalysts. (a) $\text{Co}_6\text{-Al}_3\text{S}$; (b) $\text{Co}_2\text{-Ca}_4\text{-Al}_3\text{S}$.

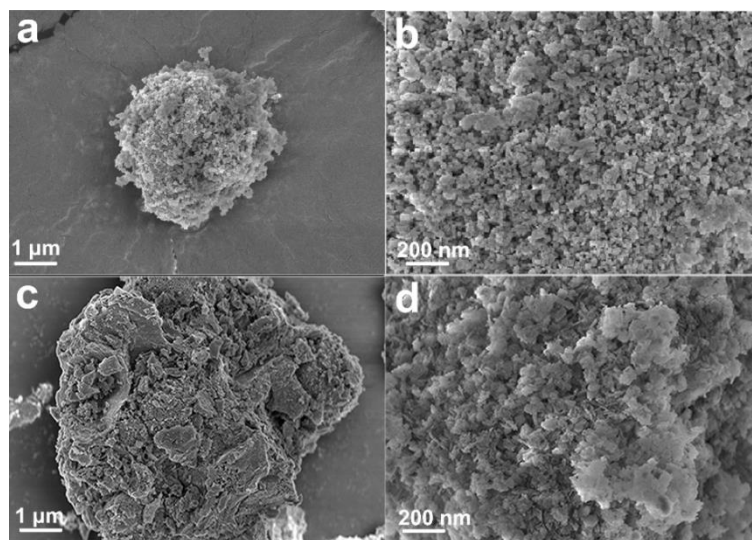


Figure S7. SEM images of the spent catalysts. (a, b) $\text{Co}_6\text{-Al}_3\text{S}$; (c, d) $\text{Co}_2\text{-Ca}_4\text{-Al}_3\text{S}$.

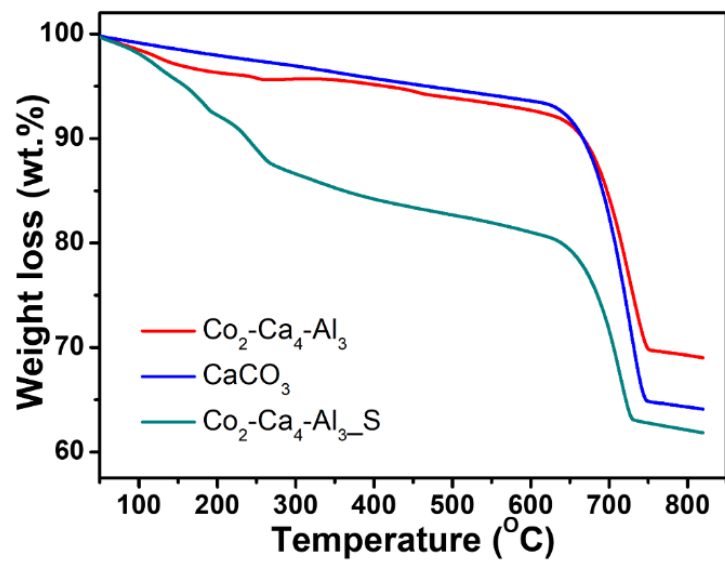


Figure S8. TGA curves of $\text{Co}_2\text{-Ca}_4\text{-Al}_3$, CaCO_3 and $\text{Co}_2\text{-Ca}_4\text{-Al}_3\text{-S}$.

Table S2. Comparison of the Co₂-Ca₄-Al₃ catalyst with those reported catalytic systems in the selective hydrogenolysis of glycerol.

Catalyst	Reaction conditions	Yield of 1,2-PDO (%)	Run numbers	TOS (h) ^a	Ref.
Cu/ZrO ₂	4 wt % glycerol aqueous solution, 200 °C, 10 h, 2.5 MPa H ₂	32.7	3	n.d.	1
Cu-Pd/TiO ₂ -Na	20 wt % glycerol aqueous solution, 220 °C, 6 h, 0.7 MPa H ₂	55.3	4	n.d.	2
ZnPd/ZnO@Al ₂ O ₃	20 wt % glycerol aqueous solution, 230 °C, 6 h, 3 MPa H ₂	74.2	5	n.d.	3
8Ce/Cu-Co-Al	20 wt % glycerol ethanol solution, 230 °C, 3.5 MPa H ₂	84.6	n.d.	100	4
PdZn/ZnAl ₂ O ₄	10 wt % glycerol aqueous solution, 220 °C, 4 h, 5 MPa H ₂	31.5	10	n.d.	5
Cu _{0.1} -Mg _{0.2} /SiO ₂	20 wt % glycerol aqueous solution, 210 °C, 24 h, 4.5 MPa H ₂	82.8	5	n.d.	6
8Nb/Pd-Zr-Al	10 wt % glycerol aqueous solution, 200 °C, 8 h, 3.5 MPa H ₂	58.5	4	n.d.	7
Ru/Mg(OH) ₂ (S)	4.2 wt % glycerol aqueous solution, 210 °C, 2 h, 3 MPa H ₂	15.8	5	n.d.	8
PtIn-2	10 wt % glycerol ethanol solution, 220 °C, 12 h, 2 MPa H ₂	90.9	5	n.d.	9
5CuO/Ga _{2.3} -HT	20 wt % glycerol aqueous solution, 220 °C, 0.5 MPa H ₂	92.2	n.d.	23	10
Co ₂ -Ca ₄ -Al ₃	20 wt % glycerol aqueous solution, 210 °C, 10 h, 4 MPa H ₂	90.5	6	280	This work

^aTOS: time on stream.

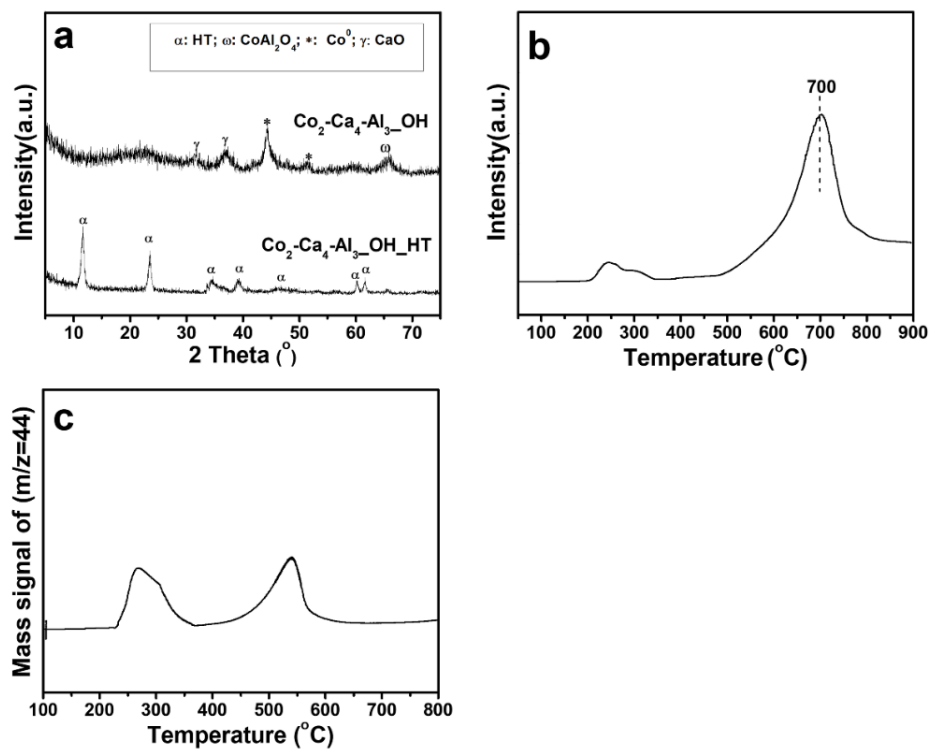


Figure S9. (a) XRD patterns of the $\text{Co}_2\text{-Ca}_4\text{-Al}_3\text{-OH}_{\text{HT}}$ and $\text{Co}_2\text{-Ca}_4\text{-Al}_3\text{-OH}$. (b) H_2 -TPR profiles of the $\text{Co}_2\text{-Ca}_4\text{-Al}_3\text{-OH}_{\text{HT}}$. (c) CO_2 -TPD profiles of $\text{Co}_2\text{-Ca}_4\text{-Al}_3\text{-OH}$ catalyst.

Table S3. The hydrogenolysis of glycerol on various catalysts by controlling the reaction conditions.^a

Entry	Catalysts	Con. (%)	Sel. (%)				
			1,2-PDO	EG	DHA	LA	Others ^e
1	Co ₂ -Ca ₄ -Al ₃	73.0	91.0	2.7	-	2.3	4.0
2	Co ₂ -Ca ₄ -Al ₃ _OH	76.5	74.4	3.5	-	13.5	8.6
3	Co ₂ -Ca ₄ -Al ₃ _Ox	6.0	5.5	2.3	-	77.0	15.2
4	Co ₂ -Ca ₄ -Al ₃ _Ox ^b	3.5	4.0	1.5	-	74.5	20.0
5	Co ₂ -Ca ₄ -Al ₃ ^b	23.0	47.3	12.5	-	26.5	13.7
6	Co ₂ -Ca ₄ -Al ₃ ^c	13.5	-	-	69.0	10.5	20.5
7	Co ₂ -Ca ₄ -Al ₃ ^d	100	58.0	3.5	-	2.5	36.0

^aReaction conditions: 15.0 mL 20 wt % glycerol aqueous solution, 0.5 g catalyst, 4.0 MPa H₂, 210°C, 5 h unless indicated otherwise. ^bThe reaction was carried out under N₂ atmosphere (1.0 MPa). ^cThe reaction was carried out under N₂ atmosphere (1.0 MPa), 80°C, 24 h. ^d20 wt % of DHA aqueous solution was used as substrate. ^eOthers: CO₂, CO, CH₄, MeOH, 2-PO and other unidentified products. 1,2-PO: 1,2-propanediol; EG: ethylene glycol; DHA: Dihydroxyacetone; 2-PO: 2-propanol.

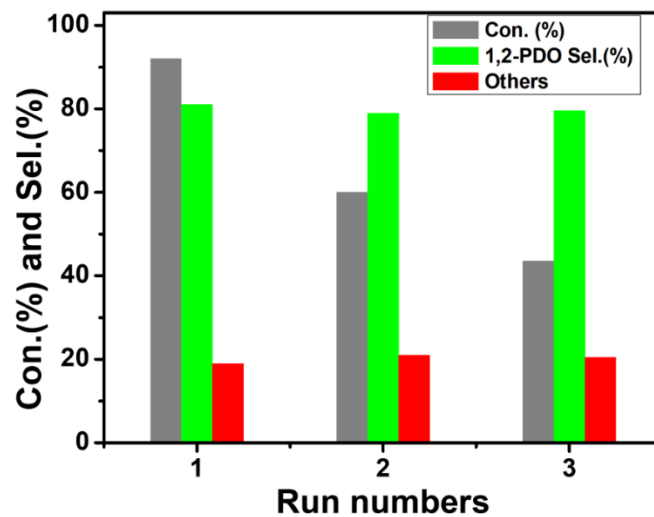


Figure S10. The recyclability of $\text{CO}_2\text{-Ca}_4\text{-Al}_3\text{-OH}$ catalyst for selective hydrogenolysis of crude glycerol. Others: EG, MeOH, 2-PO, LA, CO_2 , CO, CH_4 and other unidentified products. Reaction conditions: 15.0 mL crude glycerol aqueous solution (50.2 wt %), 0.5 g catalyst, 4.0 MPa H_2 , 210 °C, 10 h.

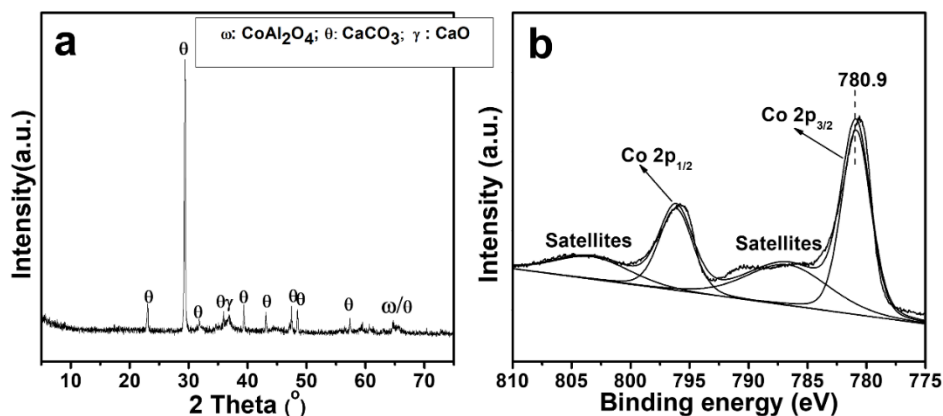


Figure S11. (a) XRD patterns of the $\text{Co}_2\text{-Ca}_4\text{-Al}_3\text{-Ox}$ catalyst; (b) Co 2p XPS spectrum of the $\text{Co}_2\text{-Ca}_4\text{-Al}_3\text{-Ox}$ catalyst.

References

- (1) Gabrysch, T.; Peng, B.; Bunea, S.; Dyker, G.; Muhler, M. The Role of metallic copper in the selective hydrodeoxygenation of glycerol to 1,2-propanediol over Cu/ZrO_2 . *ChemCatChem* **2018**, *10*, 1344–1350, DOI: 10.1002/cctc.201701748.
- (2) Ardilaa, A.; Sánchez-Castillo, M.; Zepedad, T.; Villae, A.; Fuentes, G. Glycerol hydrodeoxygenation to 1,2-propanediol catalyzed by $\text{CuPd/TiO}_2\text{-Na}$. *Appl. Catal. B: Environ.* **2017**, *219*, 658–671, DOI: 10.1016/j.apcatb.2017.08.006.
- (3) Li, X.; Zhang, B.; Wu, Q.; Zhang, C.; Yu, Y.; Li, Y.; Lin, W.; Cheng, H.; Zhao, F. A facile strategy for confining ZnPd nanoparticles into a $\text{ZnO@Al}_2\text{O}_3$ support: A stable catalyst for glycerol hydrogenolysis. *J. Catal.* **2016**, *337*, 284–292, DOI: 10.1016/j.jcat.2016.01.024.
- (4) Cai, F.; Xiao, G. Promoting effect of Ce on a Cu-Co-Al catalyst for the hydrogenolysis of glycerol to 1,2-propanediol. *Catal. Sci. Technol.* **2016**, *6*, 5656–5667, DOI: 10.1039/c6cy00116e.
- (5) Zhang, X.; Liu, C.; Ke, C.; Liu, L.; Hao, X.; Wu, Y.; Wan, S.; Wang, S.; Wang, Y. Hydrothermally stable ZnAl_2O_4 nanocrystals with controlled surface structures for the design of long-lasting and highly active/selective PdZn catalysts. *Green Chem.* **2019**, *21*, 6574–6578, DOI: 10.1039/c9gc02483b.
- (6) Kumar, P.; Shah, A.; Lee, J.; Park, Y.; Štanger, U.; Selective hydrogenolysis of

glycerol over bifunctional copper-magnesium-supported catalysts for propanediol synthesis. *Ind. Eng. Chem. Res.* **2020**, *59*, 6506–6516, DOI: 10.1021/acs.iecr.9b06978.

(7) Cai, F.; Jin, F.; Hao, J.; Xiao, G. Selective hydrogenolysis of glycerol to 1,2-propanediol on Nb-modified Pd-Zr-Al catalysts. *Catal. Commun.* **2019**, *131*, 105801, DOI: 10.1016/j.catcom.2019.105801.

(8) Liu, J.; Ruan, L.; Liao, J.; Pei, An.; Yang, K.; Zhu, L.; Chen, B. Magnesium hydroxide-supported ruthenium as an efficient and stable catalyst for glycerol-selective hydrogenolysis without addition of base and acid additives. *New J. Chem.* **2020**, *44*, 16054–16061, DOI: 10.1039/d0nj03157g.

(9) Zhang, X.; Cui, G.; Wei, M. PtIn alloy catalysts toward selective hydrogenolysis of glycerol to 1,2-propanediol. *Ind. Eng. Chem. Res.* **2020**, *59*, 12999–13006, DOI: 10.1021/acs.iecr.0c02299.

(10) Mittaa, H.; Devunurib, N.; Sunkaric, J.; Mutyalad, S.; Ballae, P.; Perupogua, V. A highly active dispersed copper oxide phase on calcined $\text{Mg}_9\text{Al}_{2.7}\text{-Ga}_{2.3}\text{O}_2$ catalysts in glycerol hydrogenolysis. *Catal. Today* **2020**, DOI: 10.1016/j.cattod.2020.02.032.